energy&fuels

pubs.acs.org/EF Article

Combustion and Flame Front Morphology Characterization of H_2−CO Syngas Blends in Constant Volume Combustion Bombs

M. Reyes,* F.V. Tinaut, B. Giménez, and A. Camaño

Cite This: *Energy Fuels* 2021, 35, 3497−3511 Read Online

ACCESS | Metrics & More | Article Recommendations

ABSTRACT: The need to develop new, alternative, and bio-origin fuels for use in internal combustion engines has motivated the realization of this research, which aims to characterize the combustion process synthesis gas, represented by H_2−CO blends, which are its main constituents. Syngas can be considered a biofuel because it is a mixture of carbon monoxide, hydrogen, and other hydrocarbons, and it is formed by partial combustion of biomass. Experimental tests have been developed in two constant volume combustion bombs with spherical and cylindrical geometries to analyze the combustion process and the influence of the blend composition on the burning velocity. In the first one, the pressure registered during the combustion has been used to obtain the mass burning rate, temperatures, and burning velocities. The cylindrical bomb has two optical accesses through which the combustion process can be visualized and recorded with the Schlieren technique, and it has been used to characterize the morphology of the flame, the evolution of the flame front, or the laminar burning velocities, among other parameters of interest in the combustion process. For initial conditions of 0.1 MPa and 300 K, blends with different compositions and equivalence ratios have been studied. The introduction of hydrogen enhances combustion velocity and pressure, introducing also instabilities visible on flame front images, similar effects to those produced by increasing the equivalence ratio. Regarding the morphology of the flames, note that the tend to wrinkle and the cellularity increases as the hydrogen content of the mixture increases and the equivalence ratio decreases. The dependence of the numerical values of burning velocity has been expressed as a correlation on pressure and temperature. Finally, comparing the results of the burning velocities obtained in the spherical bomb and in the cylindrical bomb with those of different authors of the bibliography has checked the consistency and validity of them. Results of syngas blends are essential for the validation, optimization, and development of kinetic models for combustion development.

1. INTRODUCTION

Traditionally the fuels used in internal combustion engines (ICE) are derived from petroleum, therefore being of fossil origin. In spark ignition engines (SIE) gasoline is used, while in compression ignition engines (CIE), the fuel used is diesel. Its state of aggregation is liquid, which facilitates storage in environmental conditions and, due to its high energy density, gives the engine great autonomy with a relatively simple power system. These, and other more specific advantages of each type of engine, make these fuels very interesting for use in RICE in general, and for consumption in the automotive sector in particular.[1] Since the first ICE was developed, properties of fuels have evolved due to various factors: oil prices, the progress of refinery processing technologies, the development of engine technology, the requirements of vehicle performance and control, and, more recently, environmental regulations that seek to reduce the impact of polluting gases with the improvement of its technologies and processes.

Fossil fuels are the basis of the modern industry, being also widely used in all areas of life, which makes them a vital element of the world economy. However, the limited type of fossil fuel resources leads to their depletion, rising oil prices, and the energy dependence of producing countries. In addition, its combustion has a negative impact on the environment and people's health. All this together make it necessary to find new clean energies, as well as improving the efficiency of combustion processes.

One of the solutions to the above problems is the development of alternative fuels and biofuels, produced through different processes from biomass, which are becoming increasingly important.

Gaseous fuels are preferred to liquid and solid fuels because pollutant emissions from combustion devices operated with gaseous fuels can be controlled more easily because they contain no mineral impurities and are easier to burn, thus achieving greater efficiencies. As for the feeding system, it is less expensive to produce and operate than other types of fuels.[2] In addition, they have a high hydrogen/carbon ratio, so they produce low carbon-based emissions, such as CO or CO_2.[3] On the contrary, the gaseous state of fuels implies that the energy density per unit volume, or mass unit including the pressure tank, is lower than that of liquid fuels. This implies that the storage system requires more space, which is very

Received: October 27, 2020
Revised: January 4, 2021
Published: January 28, 2021

https://dx.doi.org/10.1021/acs.energyfuels.0c03598
Energy Fuels 2021, 35, 3497−3511

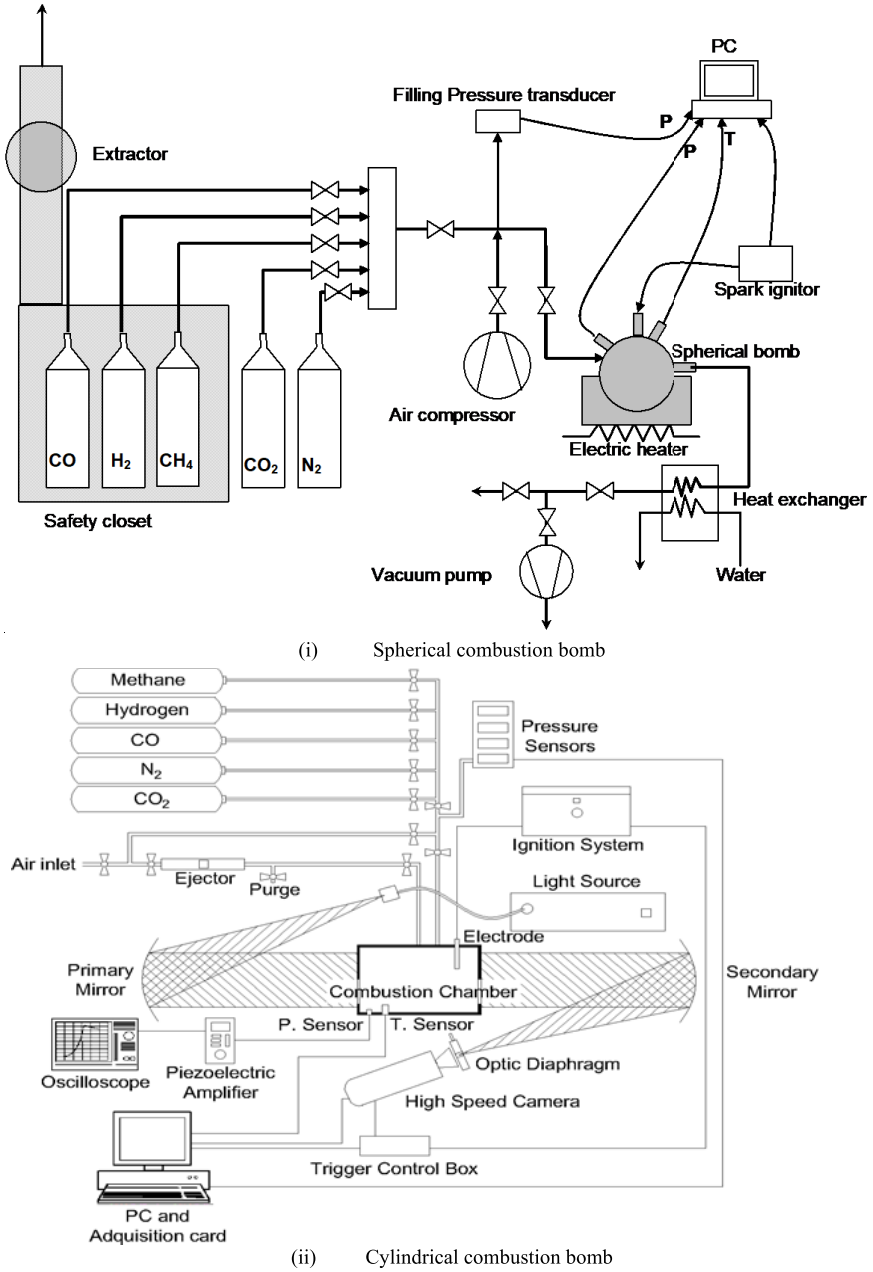

Figure 1. Schemes of the experimental setups.

limited in cars, and a decrease in the autonomy of the vehicle itself.

The most commonly used gaseous fuels are natural gas (NG) and liquefied petroleum gas (LPG). Even so, the most interesting alternative gaseous fuels, being of renewable and/or residual origin (Renewable and Residual Fuels, RRF), are hydrogen (H_2), biogas (CH_4–CO_2), and synthesis gas (H_2–CO).

Hydrogen (H_2) is a colorless, odorless, and non-toxic gas. It burns with an invisible flame and without smoke since the products of its combustion consist mainly of water and some nitrogen oxides (NOx). Even so, in the combustion products there may be traces of CO, CO_2, and HC because of the burning of the lubricating oil. The octane number of H_2 (106) is higher than that of gasoline (>95), making it more suitable for SIE, due to its higher anti-knock rate. However, H_2 has a very low ignition energy, which is one of the problems for combustion applications. The laminar burning velocity of H_2 is approximately 10 times more than that of gasoline or methane. This faster combustion implies lower thermal losses in the engine and therefore an increase in its efficiency.[4,5] Its flammability limits are very wide, from 5 to 75% in volume, which allows working with poor mixtures. The most common way of obtaining hydrogen is by electrolysis of water using renewable sources (solar, wind, hydraulic), thus using pollution-free electricity.[2] This fuel is a very interesting option to achieve the goal of global decarbonization, given that its global warming potential is negligible. However, the use of pure hydrogen in internal combustion engines presents a series of difficulties in terms of safety, storage, and economy. Several investigations, such as those of Karim[6] or Verhelst and Sierens,[7] found that using pure hydrogen favored self-ignition of the mixture, especially for higher engine loads. In addition, there is an increase in NO_x emissions because of the higher

https://dx.doi.org/10.1021/acs.energyfuels.0c03598
Energy Fuels 2021, 35, 3497−3511

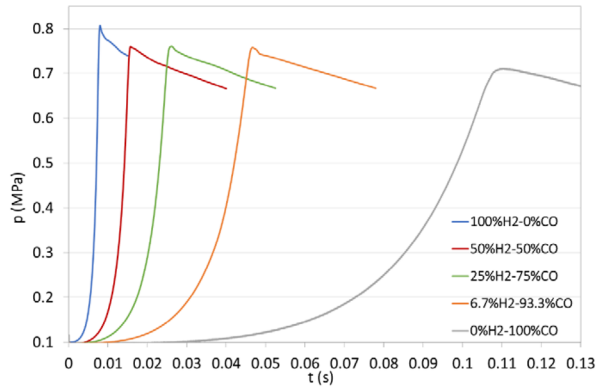

(i)

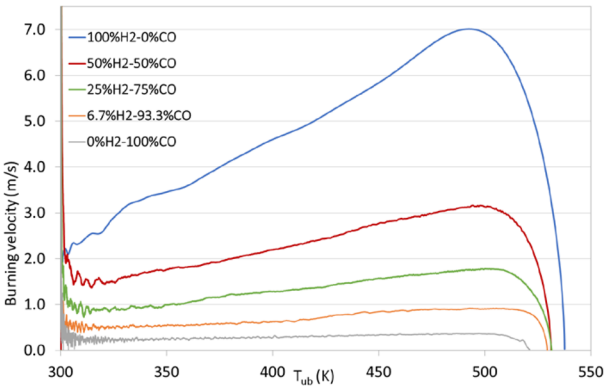

(ii)

Figure 2. Influence of mixture composition on the pressure evolution (i) and burning velocity (ii), in the spherical bomb for stoichiometric equivalence ratio, and 0.1 MPa and 300 K initial conditions.

flame temperature. That is why the strong reactivity and wide flammability limits, together with the problems derived from the combustion of pure hydrogen, make hydrogen an ideal fuel to combine with others with slower burning velocity and narrow ranges of operational mixing. Therefore, hydrogen can be defined as a combustion enhancer, significantly accelerating the rates of flame propagation, extending the range of poor operating mix and thus reducing CO_2 emissions. Ji and Wang[8] confirmed how enrichment of gasoline with H_2 in an SIE can improve performance and increase engine torque at low loads and low engine speed. They also verify that HCs decreased, while NO_x increased as hydrogen enrichment increased. In addition, there are numerous studies about the enrichment of natural gas with hydrogen (HNG). NG is a mixture of different gases with methane as its main components. With the mixture of both fuels, for poor mixtures, engine performance can be improved and CO and HC emissions can be lowered by adding small amounts of hydrogen in NG.[9] In general, CO, CO_2, and HC emissions decrease as the proportion of hydrogen in the NG increases; on the contrary, NO_x emissions increase due to the higher combustion rate, and in turn to the increase in the combustion temperature of the mixture.[10] On the other hand, Das et al.[11] compared the performance and combustion characteristics of an H_2-powered and compressed natural gas (CNG) engine, showing better thermal efficiency for the H_2 case after.

In summary, H_2 has great potential as a fuel in ICE. However, there are different obstacles that today impede its full development. These include the lack of production, distribution, and the necessary storage infrastructure. There are some methods for production of hydrogen from hydrocarbons, usually as a mixture with carbon monoxide, which is called syngas. An example is to process coal into syngas with the gas generator—the water gas method;[12] coal distillation and gasification are also used to obtain hydrogen with other gases (CO, CO_2, etc.).

Several authors have studied the behavior of synthesis gas in ICE[8,13] and verified that with an increase in H_2 concentration and a decrease in CO, a higher thermal efficiency of the engine was obtained, as well as a decrease in NO_x and HC. Other research lines[14,15] try to compare the behavior of syngas in contrast to other fuels in an SIE.

Authors such as Lee et al.,[16] Bouvet et al.,[17] Dong et al.,[18] Fu et al.,[19] or Sun et al.[20] investigated the laminar burning velocity of syngas flames for mixtures with different proportions of H_2−CO with atmospheric conditions. All of them reported that the burning velocity increases as the proportion of hydrogen increases in the mixture. Hassan et al.[21] studied the effects of positive flame stretch on the laminar burning velocities of H_2/CO−air mixtures for outwardly propagating spherical flames for concentrations of H_2 in the mixture ranging from 3 to 50% (by volume) in a spherical windowed chamber and computationally. Natarajan et al.[22] investigated laminar flame speeds of lean H_2/CO/CO_2 (syngas) fuel mixtures by using images of the flame area in a conical Bunsen flame and based on measurements of the velocity profile in a one-D stagnation flame, compared results with numerical predictions. Singh et al.[23] measured laminar flame steeds of premixed syngas−air mixtures using a spherically expanding flame configuration for different fuel/air equivalence ratios (0.6−3.0), H_2 content, and initial temperatures. They also studied the effect of the addition of H_2O to syngas to understand the effect of moisture in coal-derived syngas. He et al.[24] studied the effect of the variation of CO content on the syngas laminar burning velocity by using the heat flux method and comparing results with a kinetic model. They obtain a linear increment on the laminar burning velocity of syngas when the content of H_2 is 25%. Jiang et al.[25] measured the laminar and turbulent burning velocities at various hydrogen proportions and the promotion of turbulence on the burning velocity for different fractions of hydrogen. The effect of hydrogen fraction on flame inherent instabilities and on self-acceleration propagation was studied in ref 26. The self-similar propagation of a turbulent expanding flame, H_2/CO/air mixtures, was also investigated in ref 27.

A few works have investigated the syngas burning velocity at high pressures conditions (up to 2 MPa), highlighting those of Sun et al.,[20] Sikes et al.,[28] and Kéromnès et al.[29] In these studies, O_2 diluted in He was used instead of air (N_2 and O_2) as oxidant, in a 1:7 ratio. In this way, it is possible to reduce the high cellularity of the flames, due to the high pressures, and thus be able to easily measure the burning velocity. All these studies show that the burning velocity decreases when pressure of the mixture increases.

Among the also few studies about the influence of the preheating temperature of the mixture on the burning velocity, the studies of Sun et al.,[20] Sikes et al.,[28] and Kéromnès et al.[29] can be found, which reached temperatures between 300 and 700 K. They all came to the same conclusion: the preheating temperature of the mixture substantially increases the speed of the flame. The effect of dilution of N_2 and CO_2 in the syngas has been established, since, in practice, they are components

https://dx.doi.org/10.1021/acs.energyfuels.0c03598
Energy Fuels 2021, 35, 3497−3511

that are part of the fuel. Prathap et al.[30] and Burbano et al.[31] investigated the laminar burning velocity of 50% H_2−50% CO mixtures diluted with 20, 40, and 60% N_2, concluding that the addition of nitrogen substantially decreases the maximum combustion rate, displacing this peak toward poorer mixtures. On the other hand, Wang et al.[32] focused on the effect of dilution with various CO_2 ratios. They observed that the dilution of carbon dioxide reduces the speed of the flame more intensely than nitrogen due to the dissociation of carbon dioxide during combustion.

There are also investigations that analyze the influence of ignition energy on the laminar burning velocity, focused on finding the critical radius of the flame, that is, the radius from which the spread of the flame is not affected by the energy of the spark. Bradley et al.[33] and Huang et al.[34] observed that the ignition energy does not influence the burning velocity for flame radii bigger than 6 mm. Considering the effects of flame stretching, there are also studies on Markstein's length, which represents the sensitivity of the flame to the stretch rate. Bouvet et al.[17] summarized data on Markstein's length for syngas-air mixtures, at atmospheric pressure, from various research groups. They showed how Markstein's length decreases as pressure, temperature, or diluents (CO_2, N_2) are added to the mixture, making the flame more unstable in either case.

There are many research groups focused on the syngas combustion process, but there is not yet a sufficiently broad database, which includes all possible experimental compositions or conditions to study in detail the process. The present work goes along that line, to continue and improve the work of other investigations on the characterization of synthesis gas combustion through the flame visualization, morphological study of the flame front, expanding the tests, and results that already exist. Syngas refers to carbon monoxide/hydrogen mixtures, the building blocks to produce methanol, hydrocarbons, synthetic gasoline and diesel, or ethanol. This is the main necessity of the present work. The typical composition of the syngas, which is a function of the gasification process, includes H_2 and CO as the main burnable components with variable amounts of inert gases (CO_2, H_2) and a smaller amount of CH4. In order to characterize the combustion properties, the two main burnable components (H_2 and CO) are considered in variable proportions ranging from pure H_2 to pure CO. All ratios and percentages presented in this study are on a molar basis.

Table 1. Coefficients of the Burning Velocity Correlation for Stoichiometric Conditions

parameter	0% H_2	6.7% H_2	25% H_2	50% H_2	100% H_2
$u_{l,0}$ (m/s)	0.208	0.419	0.795	1.325	2.300
α	1.846	2.206	2.209	2.416	3.005
β	−0.20	−0.17	−0.17	−0.18	−0.19

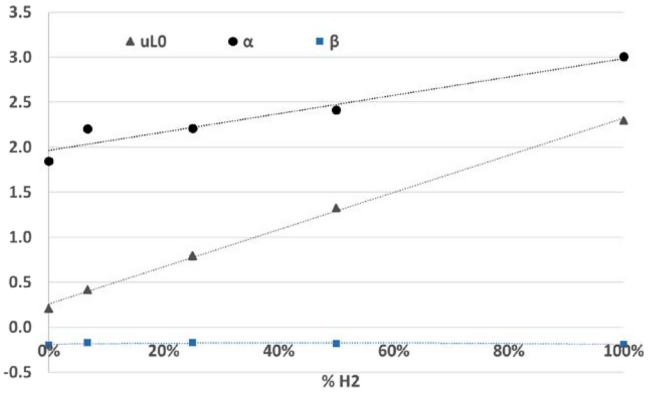

Figure 3. Evolution of the burning coefficient (uL0), and temperature (α) and pressure (β) exponents with the percentage of hydrogen in the mixture composition, in the spherical bomb for stoichiometric equivalence ratio, 0.1 MPa and 300 K initial conditions.

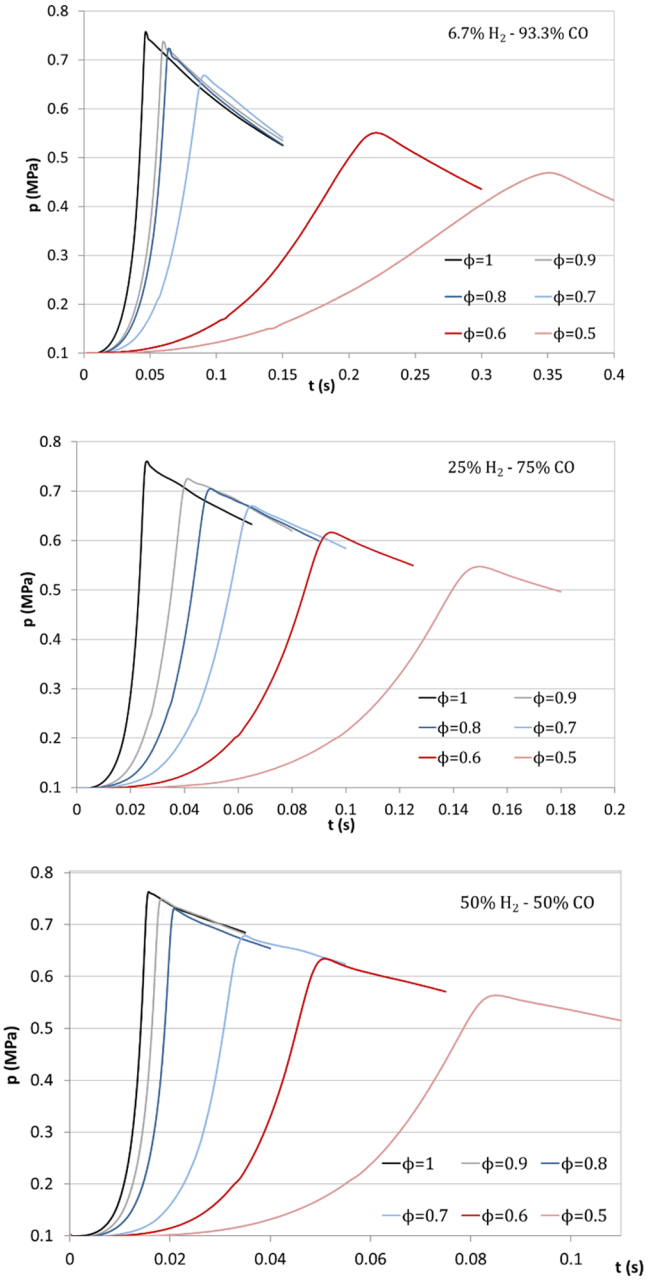

Figure 4. Influence of the fuel/air equivalence ratio on the pressure evolution of different fuel blends in the spherical bomb, for stoichiometric equivalence ratio, and initial conditions 0.1 MPa and 300 K.

2. EXPERIMENTAL SETUP

The experimental setup used in this investigation includes two different test installations designed for the study and combustion

https://dx.doi.org/10.1021/acs.energyfuels.0c03598
Energy Fuels 2021, 35, 3497−3511

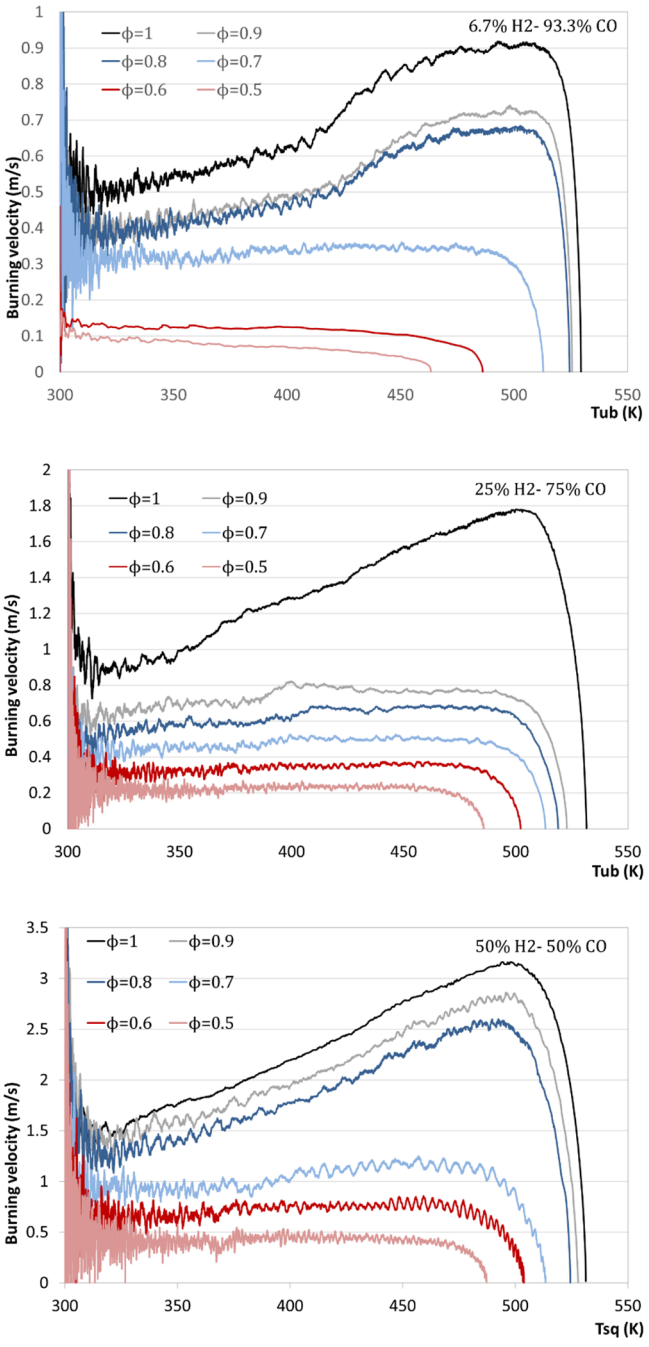

Figure 5. Influence of the fuel/air equivalence ratio on the burning velocity, versus unburned temperature for different fuel mixture compositions, in the spherical bomb for stoichiometric equivalence ratio, 0.1 MPa and 300 K.

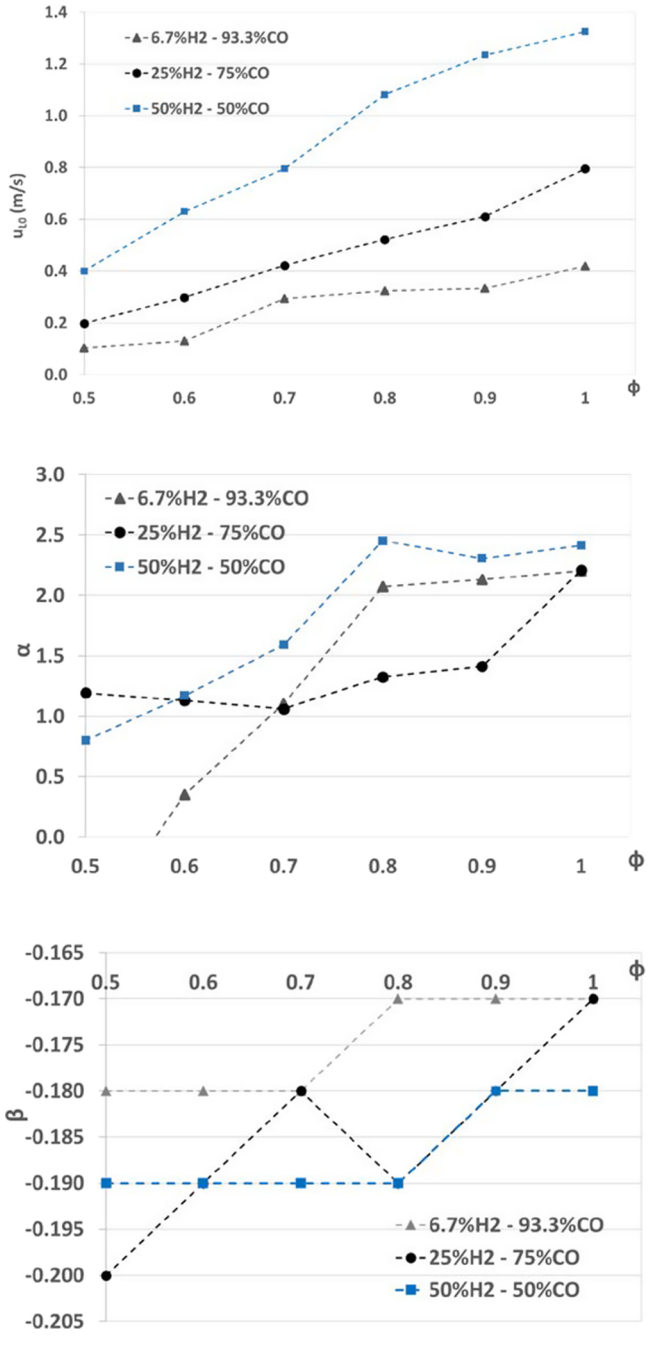

Figure 6. Coefficients u_{10}, α and β, as a function of equivalence ratio and fuel mixture composition for the pressure and temperature ranges of Table 2.

characterization of gaseous and liquid fuels. The facilities are a spherical constant volume combustion vessel (SphCVCB) and a cylindrical constant volume combustion vessel (CylCVCB). A two-zone thermodynamic diagnosis model is used to process pressure evolution inside the combustion chambers and get the combustion rate and flame velocities.

2.1. Spherical Constant Volume Combustion Bomb (SphCVCB) with a Diagnosis Combustion Model. The main components of the spherical setup are a spherical constant volume combustion chamber (SphCVCB), a system for data adquisition, and supply lines for the introduction of fuel mixture components and air. The SphCVCB spherical chamber is made of stainless steel; it has a 0.2 m diameter with a temperature and pressure transducer and two optical accesses for chemiluminescence analysis, see Figure 1i. The SphCVCB has been designed to resist pressures up to 40 MPa and temperatures up to 1073 K during the combustion development. There are two electrodes positioned at the geometric center of the SphCVCB between which the spark is discharged to start the combustion.

Before each combustion test, initial pressure, temperature, and fuel/air mixture composition have to be established. Mixtures of fuel and air are introduced in the SphCVCB; first are fuel components and later on is air, at the preferred initial conditions. To control de proportion of hydrogen in the syngas/air mixture, the filling process is made with partial pressures for each component. The equivalence ratio required in the experiment is achieved by modifying the proportions of each component in the fuel mixture. Mixing is achieved by waiting a time (5 min) to reach a homogeneous mixture inside the

https://dx.doi.org/10.1021/acs.energyfuels.0c03598
Energy Fuels 2021, 35, 3497−3511

Table 2. Coefficients and Exponents of the Burning Velocity Correlation for Different Blends with Varying Equivalence Ratios

		ϕ					
% H_2	parameter	0.5	0.6	0.7	0.8	0.9	1
6.7% H_2	$u_{l,0}$ (m/s)	0.104	0.131	0.293	0.324	0.334	0.419
	α	−0.827	0.352	1.106	2.075	2.135	2.206
	β	−0.180	−0.180	−0.180	−0.170	−0.170	−0.170
25% H_2	$u_{l,0}$ (m/s)	0.199	0.299	0.422	0.522	0.611	0.795
	α	1.194	1.133	1.062	1.327	1.415	2.209
	β	−0.200	−0.190	−0.180	0.190	−0.180	−0.170
50% H_2	$u_{l,0}$ (m/s)	0.401	0.630	0.795	1.082	1.235	1.325
	α	0.801	1.172	1.592	2.453	2.309	2.416
	β	−0.190	−0.190	−0.190	−0.190	−0.180	−0.180

combustion chamber. Once the combustion is started, a spherical flame front develops and propagates toward the outside of the SphCVCB burning and compressing the unburned mixture. During the development of the combustion, a piezoelectric transducer Kistler 7063 (maximum calibration error 0.06%) connected to a charge amplifier Kistler 5018A1000 (maximum calibration error of 0.3%) is used to register the pressure. A Yokogawa DL750 Scopecorder (16 bits AD converter) is utilized to record the output signal. The estimated error of the pressure acquisition is 0.36% over the measuring range. Additional details of the spherical experimental setup and on the complementary use of the installation and chemiluminescence emitted by OH* and CH* radicals for combustion characterization can be seen in Tinaut et al.[35] Once the combustion process is complete, the waste gas is expelled to the outside with a chimney. After this, three vacuums are made to ensure that inside the combustion bomb, there is no gas left from the previous combustions.

Temporal evolution of pressure is analyzed with a two-zone thermodynamic diagnosis model to obtain information about the combustion process such as the burning rate, burning velocities, and temperatures. The laminar burning velocity, u_l^p is calculated from the mass burning rate, $\dot{m}_b$, the unburned density ρ_{ub} and the flame front surface A_f: $u_l^p = \frac{\dot{m}_b}{\rho_{ub} \cdot A_f}$, where the burning velocity is a function of unburned temperature and pressure (note that the laminar burning velocity u_l^p is usually called u_L in the literature; here, we call it with the

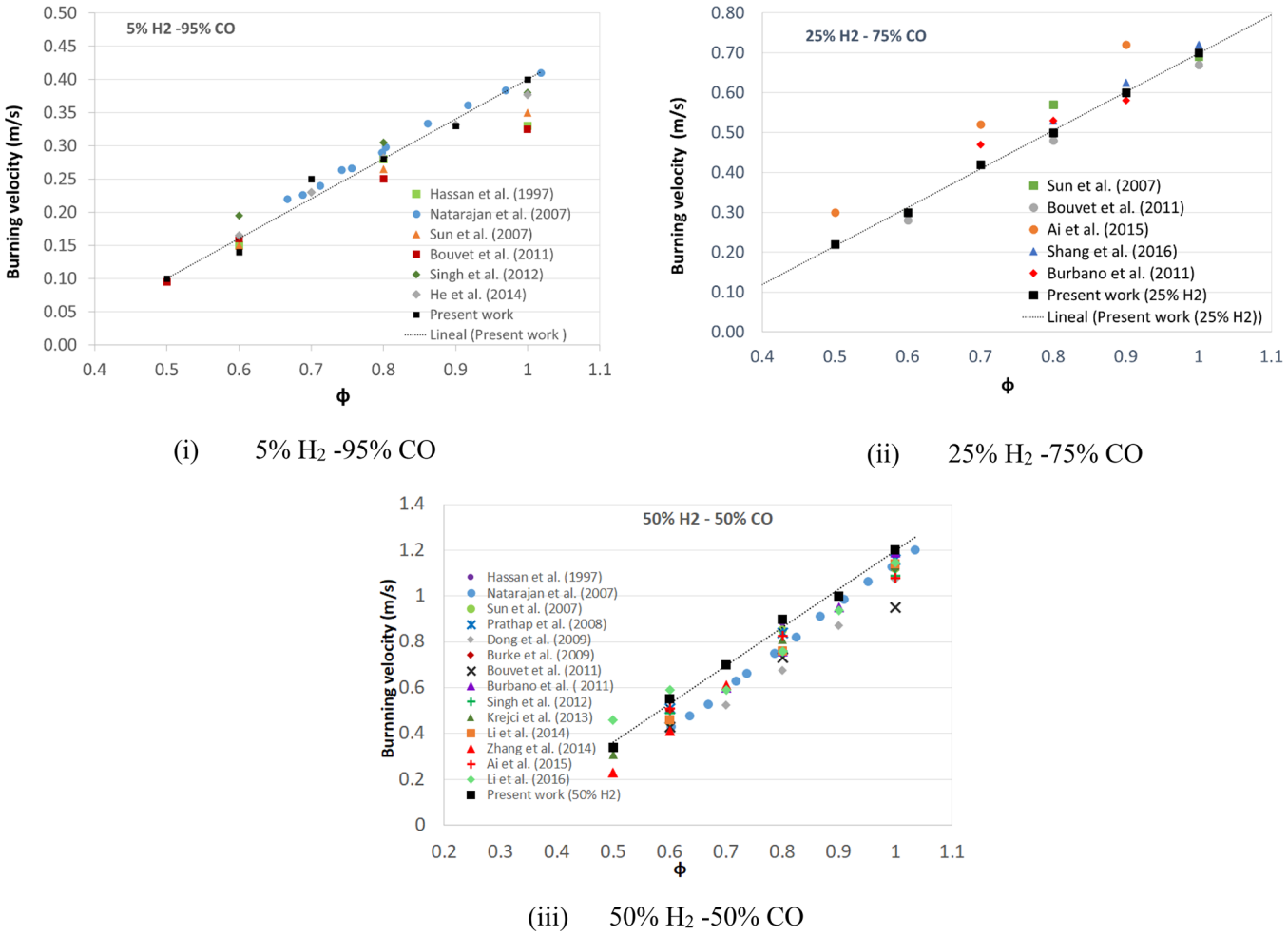

(i) 5% H_2 -95% CO (ii) 25% H_2 -75% CO

(iii) 50% H_2 -50% CO

Figure 7. Burning velocity versus equivalence ratio for 0.1 MPa and 300 K, and comparison with literature results. (i) 5% H_2 −95% CO, (ii) 25% H_2 −75% CO, (iii) 50% H_2 −50% CO.

https://dx.doi.org/10.1021/acs.energyfuels.0c03598
Energy Fuels 2021, 35, 3497−3511

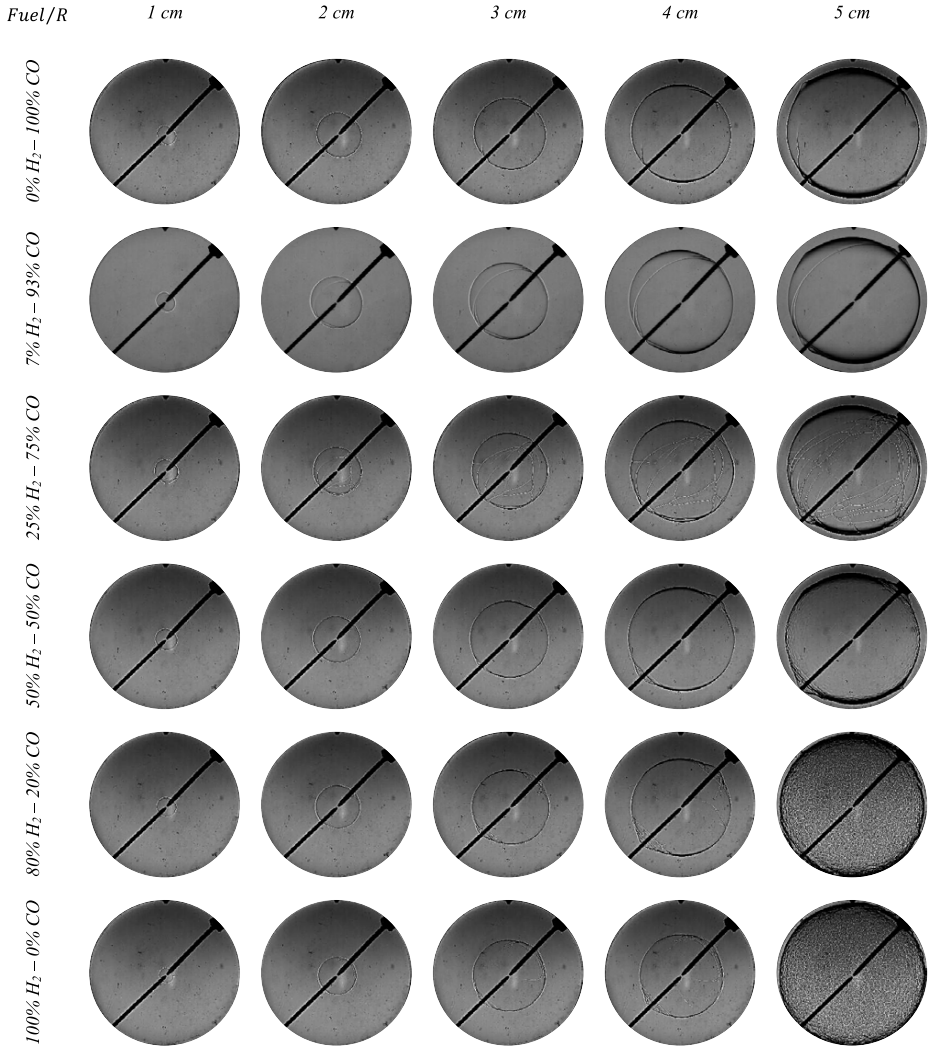

Figure 8. Schlieren images at chosen flame radii for different blend compositions (stoichiometric equivalence ratio, 0.1 MPa and 300 K).

superscript p to differentiate from the value obtained with Schlieren images technique, which we use in following sections). More details of the spherical combustion chamber and the thermodynamic analysis model can be obtained in ref 36.

2.2. Cylindrical Constant Volume Combustion Bomb (CylCVCB) with Image Acquisition. The second experimental facility used in this work to investigate the morphology and instabilities of the flame is a second combustion chamber (CylCVCB) with cylindrical geometry, with a diameter of 114 mm and a height of 135 mm to allow the study of the combustion progress and the onset of wrinkling in the flame surface. The combustion chamber has two optical windows on the sidewalls of the cylinder, both made of fused silica, to use the Schlieren technique. It is designed to resist up 40 MPa of initial pressure and 1073 K of temperature during the combustion, see Figure 1ii. The experimental device is made of a rig for the introduction of gaseous and liquid fuels, a full ignition system, and a high-speed camera Phantom V210 at 7000 frames per second (resolution 832 × 800 and exposure time 10 μs). The initial temperature is set up by electric resistances. Each fuel mixture is ignited by a spark plug at the center of the combustion chamber. The methodology for filling the cylindrical combustion bomb is the same than that explained for the spherical one. Pressure is recorded with a Kistler transducer 7063. To process the optical images obtained with the camera, an algorithm is used to obtain the flame front evolution and radius. It is well-known that under certain conditions, the flame front adopts a cellular structure, even in laminar conditions (i.e., in absence of flow turbulence) due to growth of instabilities, which occurs as a wrinkling of the flame front surface. The chamber pressure is also treated with the two-zone combustion analysis model detailed before and adapted for a cylindrical geometry. Some fluid dynamic simulations have been performed with FIRE code to predict the flame front evolution and, in particular, the deformation of the flame front due to the cylindrical geometry of the chamber.

The analysis of the sequence of flame front images, performed by means of an automated procedure (described in ref 37) allows obtaining the evolution of the flame radius R_f. The time derivative of the flame radius gives the stretched flame propagation speed S_n.[38] Plotting S_n versus flame stretch rate, α, provides a criterion to obtain the unstretched flame propagation speed, S_L, by extrapolating to a zero stretch rate.[38] $S_L - S_n = L_b \cdot \alpha$, where L_b is the Markstein length of the burned mixture. Finally, the laminar flame velocity, u_L, is computed from the S_L by considering the density ratio, $u_L = S_L \cdot (\rho_b/\rho_u)$. This velocity, u_L, obtained by means of image analysis, is consistent with the burning velocity U_L^p, obtained by means of pressure analysis. A different nomenclature is used to take into account the different way of obtaining it. According to the dynamics of premixed flames, there is a coupling between hydrodynamics and diffusion due to the variation in the gas flow velocity throughout the flame, due to the gas expansion,[39] influenced by the flame stretch rate, which has an effect on the laminar burning velocity. During the first phase of the combustion process, it could be considered that flame propagates under constant pressure condition, and then the variations in stretched flame propagation speed can be only attributed to the effect of stretch rates.

https://dx.doi.org/10.1021/acs.energyfuels.0c03598
Energy Fuels 2021, 35, 3497−3511

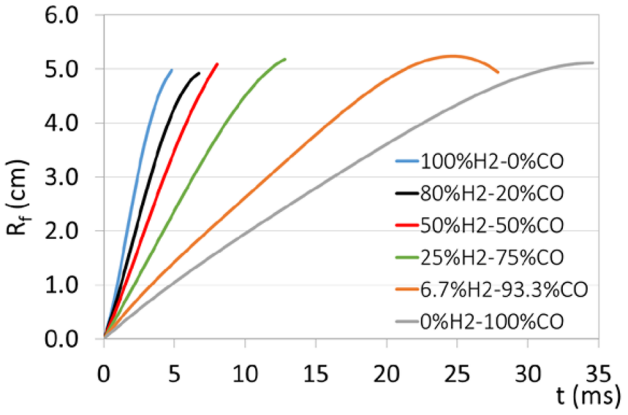

(i) Flame radius time evolution

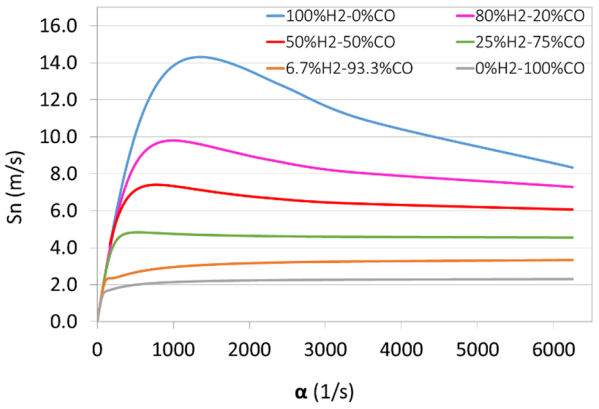

(ii) Flame speed versus stretch rate

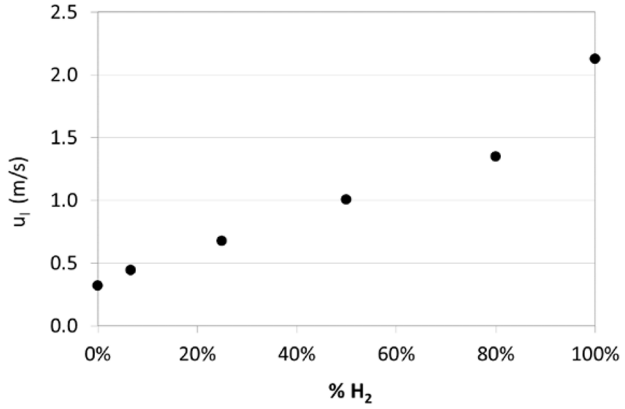

(iii) Unstretched burning velocity versus hydrogen content

Figure 9. Combustions of different H_2/CO blends at stoichiometric equivalence ratio, 0.1 MPa and 300 K initial conditions. (i) Flame radius time evolution, (ii) Flame speed versus stretch rate, (iii) Unstretched burning velocity versus hydrogen content.

3. RESULTS FROM THE SPHERICAL BOMB (SPHCVCB)

Due to the spherical geometry of the chamber, the flame front development during the combustion is not disturbed by the bomb geometry and results obtained in this bomb can be considered as reference results.

3.1. Influence of the H_2−CO Blend Composition. In this section, the influence of syngas composition (H_2−CO mixture, molar based, i.e., the content of hydrogen in the fuel mixture) on the burning velocity during the decombustion process is described.

In Figure 2i, time evolution of pressure during the combustion of different fuel mixtures is presented for mixtures from 100% of hydrogen to 100% CO. In this figure, it is possible to see the increment in the pressure as the combustion progresses inside the combustion bomb. Pressure increases progressively until the maximum value of pressure is reached, a point in which the combustion process finishes. After that point, pressure decreases. By comparing the curve of 0% H_2 (100% CO) with that of 100% H_2 (0% CO), it is possible to see that increasing the content of hydrogen in the mixture produces faster combustions, since pressure peaks are reached in shorter times. It is interesting to compare the 0 and 6.7% hydrogen lines, showing that the combustion duration for the case of 6.7% H_2 occurs in less than half the time than for the case of pure carbon monoxide. This reflects the great influence that the hydrogen content has on the burning velocity.

The corresponding burning velocities curves obtained with the two-zone thermodynamic model are represented in Figure 1ii versus the unburned temperature, which is derived from the two-zone thermochemical model. In this Figure, it is possible to directly observe the increment on the burning velocity obtained when the hydrogen content increases in the fuel mixture. The combustion-enhancing effect of hydrogen, which is reported by different authors, is confirmed in this way. In addition, observing the abscissa axis, it can be affirmed that the final temperature of the unburned mixture also slightly increases with the hydrogen content of the mixture.

The values of the burning velocity have been expressed in the form of correlations as a function of pressure and unburned temperature, following Metghalchi and Keck,[40] see eq 1. This specific correlation does not consider the changes in density and specific heat produced during the combustion. The values of the initial velocity $u_{l,0}$, the temperature exponent (α), and the pressure exponent (β) are presented in Table 1 for the different compositions, valid for pressures between 0.1 and 0.8 MPa and temperatures between 300 and 540 K.

$$u_l^p = u_{l,0} \cdot \left(\frac{T_{ub}}{T_{ub,0}}\right)^{\alpha} \cdot \left(\frac{p}{p_0}\right)^{\beta} \quad (1)$$

In Figure 3, the evolutions of $u_{l,0}$, α, and β with the H_2 content are plotted (stoichiometric conditions). In view of the

https://dx.doi.org/10.1021/acs.energyfuels.0c03598
Energy Fuels 2021, 35, 3497−3511

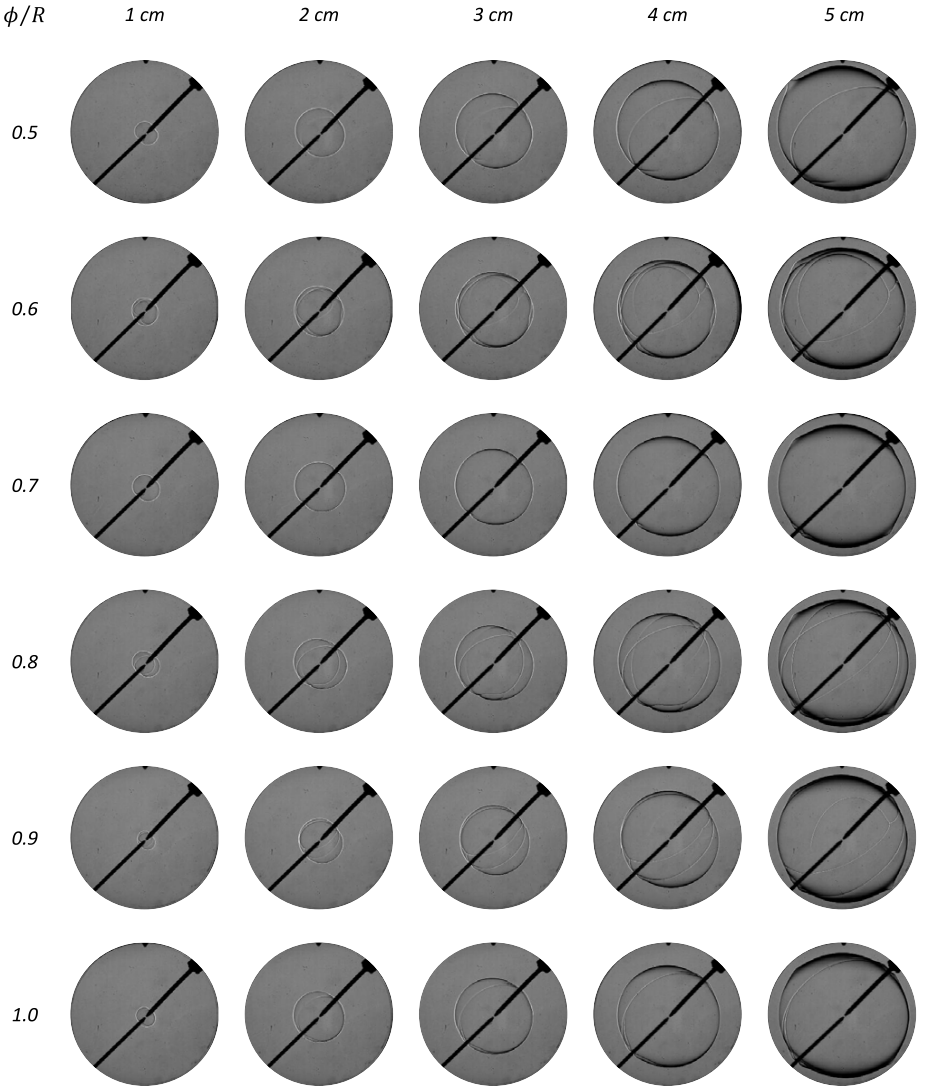

Figure 10. Schlieren images at chosen flame radii for 6.7% H_2 and 93.3% CO blend, increasing equivalence ratios, and 0.1 MPa and 300 K initial conditions.

results, several conclusions are obtained. First is that the pressure exponent (β) has a negative value, and it remains nearly constant with the variation of the composition of the mixture with an average value of −0.18. As for the value of the temperature exponent (α), a clear rising trend is shown with the percentage of hydrogen in the mixture with a minimum value for pure CO (1.846) and a maximum value for pure H_2 (3.005). The value of the burning velocity under the reference conditions ($u_{l,0}$) has the same trend, growing almost linearly with the increase of hydrogen in the mixture, having its minimum for pure CO (0.208) and its maximum for pure H_2 (2.30).

By adjusting the graphs of the different coefficients, predictive equations can be obtained for each of them, so that knowing the value of the hydrogen content in the mixture for the stoichiometric equivalence ratio and pressure and temperature initial conditions of 0.1 MPa and 300 K, each of them can be calculated, see eqs 2−4 (for pressures between 0.1 and 0.8 MPa and temperatures between 300 and 540 K).

$$u_{l,0} = 2.063 \cdot \frac{\%H_2}{100} + 0.2596 \quad (2)$$

$$\alpha = 1.018 \cdot \frac{\%H_2}{100} + 1.966 \quad (3)$$

$$\beta = -0.182 \quad (4)$$

3.2. Influence of Fuel/Air Equivalence Ratio. Figure 4 shows the time evolution of the pressure for three fuel blends, with hydrogen percentages of 6.7, 25, and 50%, with the equivalence ratio varying from 0.5 to 1. As expected, the higher the equivalence ratio, the higher final pressure and the faster combustion process are obtained for the three considered blends. It can be explained because the rate of the chemical reaction accelerates due to an increase in the fuel/air equivalence ratio of the combustion blend.

The laminar burning velocities versus the temperature of the unburned mixture, for the blends with a varying equivalence ratio, are shown in Figure 5. In accordance with the pressure plots of Figure 4, it can be seen that as the equivalence ratio increases, the burning velocity reaches its maximum for the stoichiometric mixture. It can also be seen that for lower equivalence ratios ($\leq$0.7), the burning velocity remains practically constant during combustion development, despite the fact that temperature and pressure grow. On the other

https://dx.doi.org/10.1021/acs.energyfuels.0c03598
Energy Fuels 2021, 35, 3497−3511

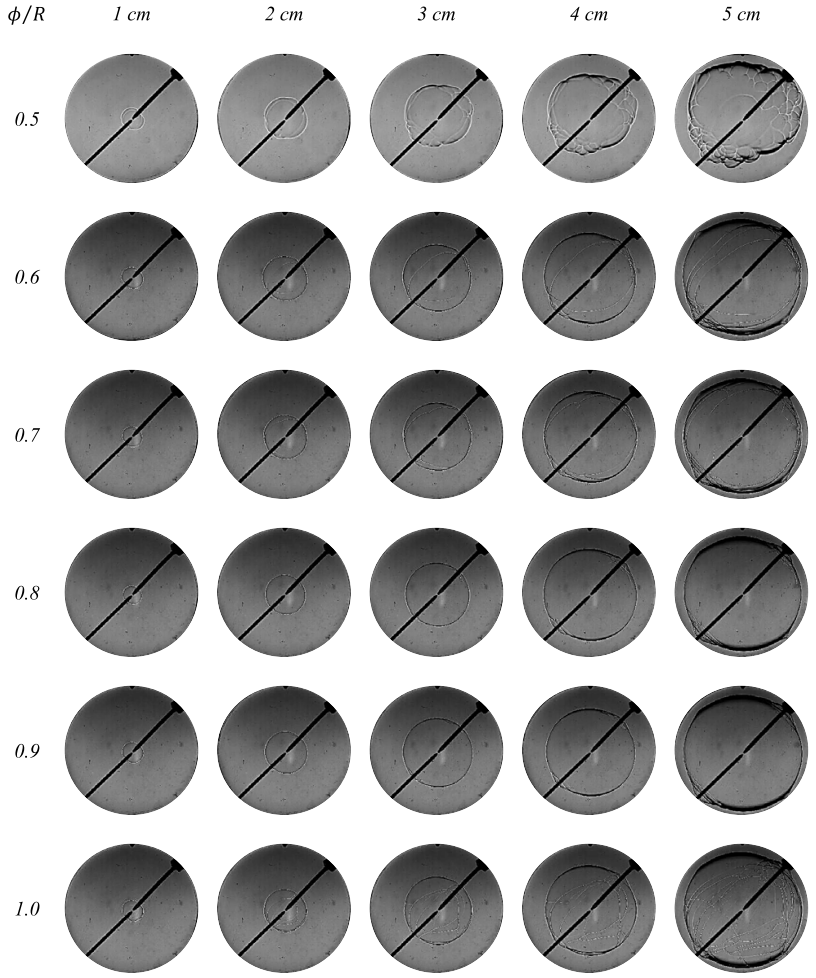

Figure 11. Schlieren images for different flame radii for a mixture of 25% H_2 and 75% CO, different equivalence ratios, and 0.1 MPa and 300 K initial conditions.

hand, the blend with 6.7% hydrogen and an equivalence ratio of 0.5 shows a decreasing evolution of the burning velocity as the temperature increases, as shown by the downward slope curve that represents it. This effect is indicative of a very slow combustion.

Once these experimental results are fitted to a Metghalchi & Keck correlation, the resulting exponents and initial coefficients are presented in Table 2, valid for pressures between 0.1 and 0.75 MPa and temperatures between 300 and 535 K. The evolution of the values of C_{c0}, α, and β of Table 2 are plotted in Figure 6.

In order to establish a comparison with other authors' results, in Figure 7, the values of the burning velocities versus the equivalence ratio are presented for three different blend compositions: Figure 7i for a mixture of 6.7% of H_2 and 93.3% CO, Figure 7ii for 25%H_2 and 75% CO, and Figure 7iii for a mixture of 50% H_2 and 50% CO. For a 5.0% H2 content, Hassan et al.,[21] Sun et al.,[20] Bouvet et al.[17] and Singh et al.[23] used a cylindrical combustion chamber, while Natarajan et al.[22] used a Bunsen burner and He et al.[24] used a heat flux burner. Since in the present work, the smallest H_2 content in the H_2−CO blend was 6.7%, an extrapolated value for 5% of H_2 has been calculated and is presented in Figure 7i.

Successively, in Figure 7ii, the burning velocities of the mixture of 25% H_2−75% CO are plotted and compared with other author values. Sun et al.[20] and Bouvet et al.[17] obtained their burning velocity values in a cylindrical combustion chamber. Han et al.[41] used a cylindrical bomb with two chambers because it supports the higher initial pressure. Burbano et al.[31] and Shang et al.[42] obtained their results in Bunsen burners. In this case, also the results obtained in the presented work agree with the rest of the results.

Finally, for the mixture of 50% H_2−50% CO, there is a larger database about the burning velocity at atmospheric conditions, see Figure 7iii. As for the experimental facilities, Sun et al.,[20] Hassan et al.,[21] Prathap et al.,[30] Bouvet et al.,[17] Singh et al.,[23] Krejci et al.,[28] Li et al.,[43] and Li et al.[44] used a cylindrical combustion bomb. Han et al.[41] and Burke et al.[45] used a cylindrical bomb with a double chamber. Natarajan et al.,[22] Dong et al.,[18] and Burbano et al.[31] obtained their values in Bunsen burners, and Zhang et al.[46] used a counterflow to obtain the burning velocity. It can be seen that regardless of the installation used, the values obtained in the present work are like the rest of the values with a bias to slightly higher values.

4. RESULTS IN THE CYLINDRICAL BOMB, CYLCVCB

With the analysis of the images obtained from the combustion process in the cylindrical bomb (using a Schlieren technique), a parametric study has been carried out in order to analyze the influence of the composition and the equivalence ratio of the mixture on the morphology of the flame (cellularity and

https://dx.doi.org/10.1021/acs.energyfuels.0c03598
Energy Fuels 2021, 35, 3497−3511

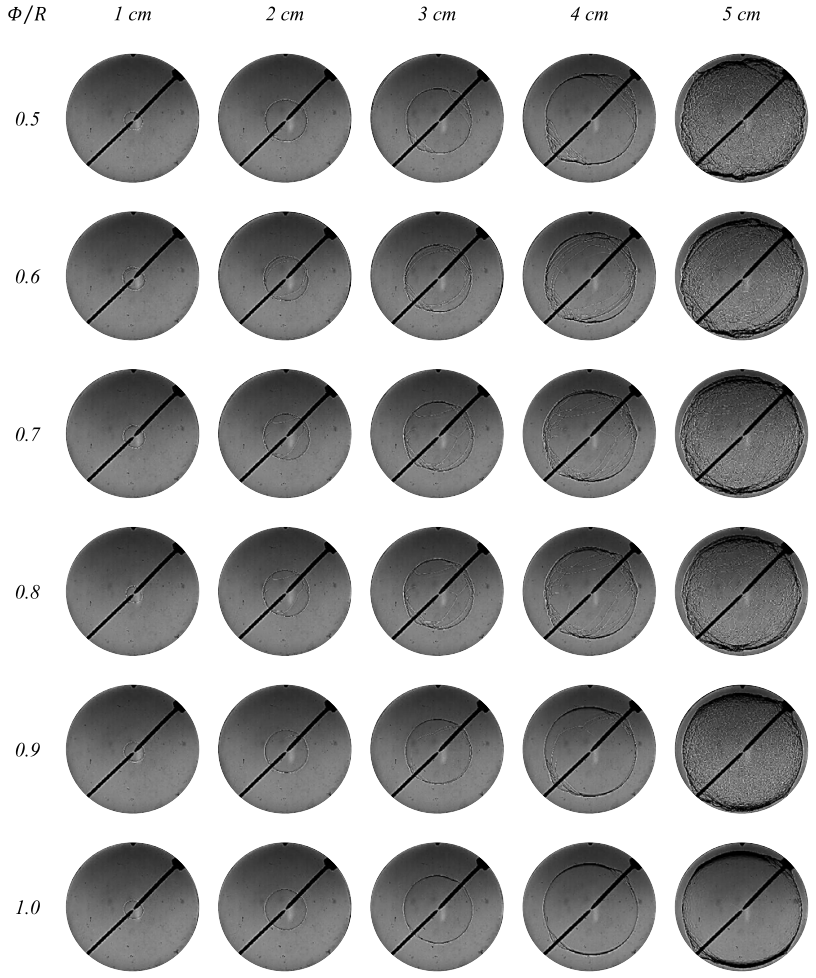

Figure 12. Schlieren images for different flame radii for a mixture of 50% H_2 and 50% CO, different equivalence ratios, and 0.1 MPa and 300 K initial conditions.

instabilities apparition), the evolution of the radius of the flame front, and its propagation speed, as well as the laminar burning velocity.

4.1. Influence of Fuel Mixture Composition. In this section, results of the Schlieren images obtained in combustion processes of different H_2/CO blends are presented when the percentage of hydrogen is varied from 0 to 100%, keeping constant the rest of parameters (stoichiometric equivalence ratio, initial pressure of 0.1 MPa, and a 300 K initial temperature). A sequence of images of the combustion at a chosen flame radius (increasing horizontally) for each fuel blend composition (increasing vertically) are presented in Figure 8. First, the sphericity of the different growing flames must be highlighted, thus checking that the hypothesis made in the two-zone diagnostic model is satisfied. Second, it is possible to see that the higher the hydrogen content in the mixture, the higher the effect of instabilities on the flame, i.e., the number of cells developed on the flame front as the combustion progresses.

Based on the evolution of the flame front images, it is possible to see that initially the flame front is smooth, which is indicative of a laminar process. It can be seen for the mixtures with 0 and 6.7% H_2 that even at the end of the combustion, the flame front remains laminar; however, the mixtures with high hydrogen contents (80 and 100%) show flame fronts with cellular surfaces. However, and for all blends, regardless of their composition, the structure of the flame front changes with the combustion progress, and the wrinkling and the apparition of instabilities increases. This last effect is clearly visualized for mixtures with higher hydrogen content (80 and 100%) and for larger flame sizes (5 cm).

In summary, it can be concluded that the hydrogen content of the fuel mixture favors the cellularity apparition and the development of instabilities in the flame front. It can be said that carbon monoxide has flames with a completely smooth and stable surface.

Figure 9 contains the plots of the flame radius time evolution (Figure 9i); the flame front speed (time derivative of the flame radius, S_l) versus stretch rate (k, Figure 9ii) is presented for combustions of different fuel mixtures for a stoichiometric equivalence ratio, an initial pressure of 0.1 MPa, and a 300 K temperature. It is possible to see that the hydrogen content accelerates the combustion process. In Figure 9ii, can be seen that these curves have, for all the compositions, a first section in which the flame speed increases significantly with the stretch rate. In the final section of all of them, it can be seen that the flame speed becomes independent of the flame front stretch rate (k), since the lines become practically horizontal. It is interesting to see that for the same stretch rate, the flame speed increases with the hydrogen content of the mixture. In addition, the hydrogen enrichment of the mixture causes the

https://dx.doi.org/10.1021/acs.energyfuels.0c03598
Energy Fuels 2021, 35, 3497−3511

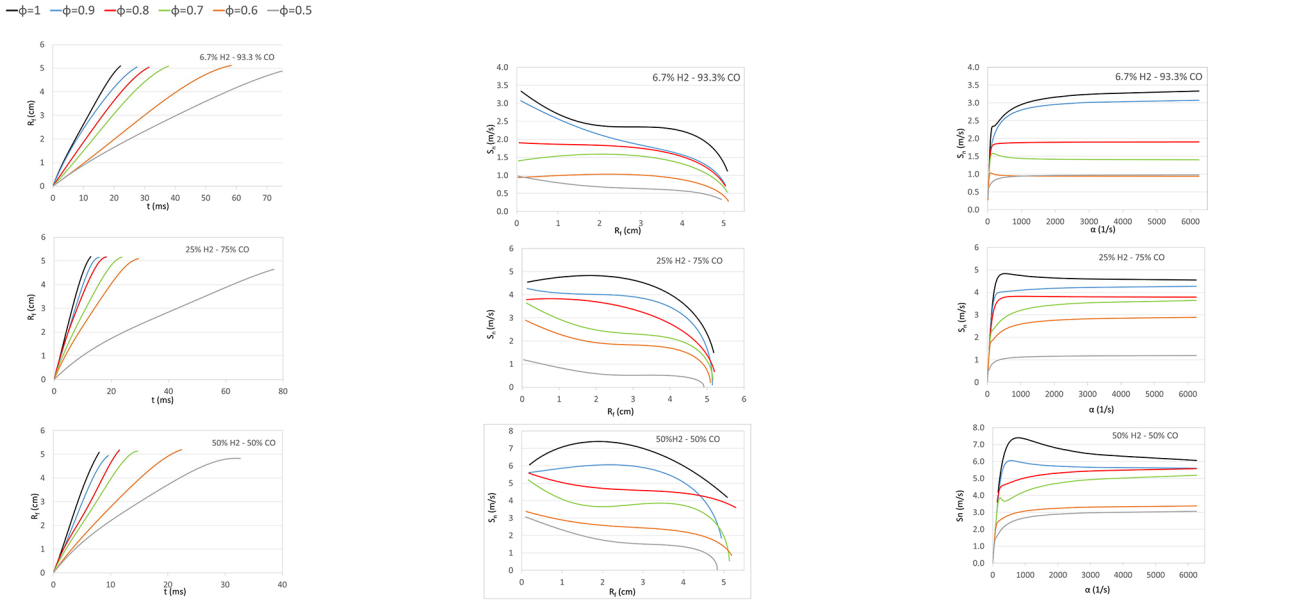

(i) Influence of fuel/air equivalence ratio on the flame radius temporal evolution in the CylCVCB, for initial 0.1 MPa and 300 K, and ϕ=0.5-1.

(ii) Influence of fuel/air equivalence ratio on the flame speed in the CylCVCB, for initial 0.1 MPa and 300 K, and ϕ=0.5-1.

(iii) Influence of fuel/air equivalence ratio on the stretched flame speed versus the stretch rate in the CylCVCB, for initial 0.1 MPa and 300 K, and ϕ=0.5-1.

Figure 13. (i) Influence of fuel/air equivalence ratio on the flame radius temporal evolution in the CylCVCB for initial conditions of 0.1 MPa and 300 K and ϕ = 0.5−1; (ii) Influence of fuel/air equivalence ratio on the flame speed in the CylCVCB for initial conditions of 0.1 MPa and 300 K and ϕ = 0.5−1; (iii) Influence of fuel/air equivalence ratio on the stretched flame speed versus the stretch rate in the CylCVCB for initial conditions of 0.1 MPa and 300 K and ϕ = 0.5−1.

displacement of the maxima to higher stretch rates that correspond to earlier stages of each combustion process.

From Figure 9ii, it is possible to obtain the unstretched burning velocity with the image method, as it was explained in section 2.2, see Figure 9iii, where values of the unstretched burning velocity versus the hydrogen content in the fuel mixture are plotted, showing a considerable increment with the hydrogen content.

4.2. Influence of Fuel/Air Equivalence Ratio. As part of the parametric study of the image analysis, the fuel/air equivalence ratio has been varied, from 0.5 to 1, maintaining constant the initial pressure and temperature, for each of the three blends (6.7, 25 and 50% H_2) considered. In the analysis on the influence of the composition on the morphology of the flame, it has been concluded that hydrogen has a destabilizing effect on the flame, causing cellularity on the flame front surface. In order to verify the effect of the equivalence ratio on the flame morphology, in Figures 10−12, the evolution of Schlieren images are represented in the form of a matrix for combustions for three different mixtures: (I) 6.7% H_2 and 93.3% CO (Figure 10), (II) 25% H_2 and 75% CO (Figure 11), and (III) 50% H_2 and 50% CO (Figure 12), in the three cases for 0.1 MPa and 300 K initial pressure and temperature, respectively.

Analyzing the Schlieren images horizontally, the evolution of the flame front for each equivalence ratio can be observed, and thus the evolution of the same flame throughout the combustion process is checked. On the other hand, following a vertical direction, the influence of the equivalence ratio on the morphology of the flame can be seen for the same radius of the flame front.

In view of the images in Figure 10, it is shown that for the fuel mixture with 6.7% H_2, no instability or cellularity appears on the flame front surface for any of the equivalence ratios analyzed. This is indicative of the fact that the hydrogen content is not high enough to cause effect on the flame instability. Sequentially, it can be said that carbon monoxide, the major component in the mixture, would have flames with a smooth and stable surface.

Based on the images of Figure 11, the effect of hydrogen on the flame morphology becomes appreciable, so that as the equivalence ratio decreases, the surface of the flame front becomes more cellular and unstable. Images of a 0.5 equivalence ratio (the lowest tested value) show the instabilizing effect of hydrogen content, especially when compared with the corresponding image sequence in the first row of Figure 10. In addition, for this same equivalence ratio, and mainly for the 4 and 5 cm flame radius, the instability phenomenon is appreciated due to the volume forces. This, as introduced in the corresponding section of the state of the art, is motivated by the strong difference in densities between the fresh mixture and the burnt gases, giving that sense of buoyancy in the flame. This phenomenon, however, is evident only in cases where the laminar burning velocity is low, associated to small equivalence ratios.

When the fuel mixture contains an important amount of hydrogen, 50%, in Figure 12, the destabilizing effect is clearly appreciated. Being very representative for the 5 cm flame radius, it can be affirmed that the roughness and instability of the flame front surface is increased with the decrease of the equivalence ratio, as already observed for the mixture with 25% hydrogen. In addition, also in this case, the flames at the beginning of their propagation have a smooth surface, and as the flame grows in size, they get a more irregular surface.

Figure 13 shows the temporal evolution of the radius of the flame front. In general, it can be affirmed that increasing the equivalence ratio of the fuel mixture increases the laminar flame speed, as expected.

Within the lines belonging to the mixture of 25% H_2−75% CO, the one corresponding to the 0.5 equivalence ratio stands out because it differs from those of the other equivalence ratios. This curve corresponds to the one mentioned in the

https://dx.doi.org/10.1021/acs.energyfuels.0c03598
Energy Fuels 2021, 35, 3497−3511

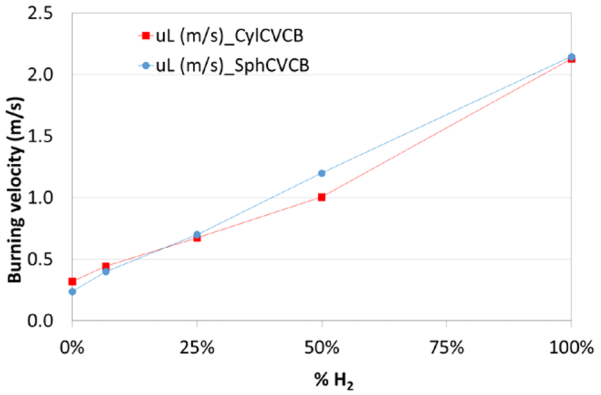

(i) Influence of the mixture composition for stoichiometric conditions

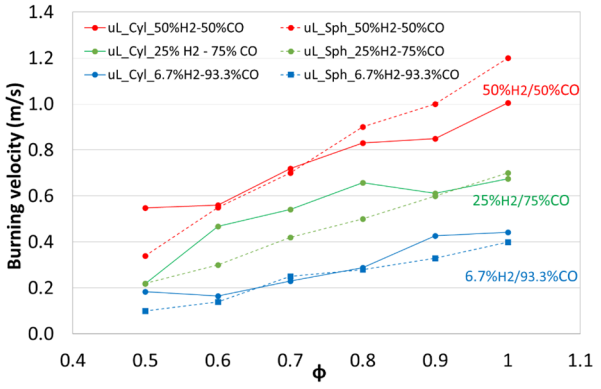

(ii) Influence of the equivalence ratio

Figure 14. Comparison between the burning velocity in the SphCVCB (u_l^p) with the values obtained in the CylCVCB (u_l), for stoichiometric equivalence ratio, 0.1 MPa and 300 K initial conditions. (i) Influence of the mixture composition for stoichiometric conditions. (ii) Influence of the equivalence ratio.

previous section with pronounced cellularity, in addition to the phenomenon of instability due to volume forces. For these reasons, the evolution of the flame front occurs slower than for the rest of equivalence ratios.

From the representation of the flame speed with respect to the radius of the flame front, it can be deduced that for the same size of the flame front, the flame speed increases as the equivalence ratio does, see Figure 13ii. In general, for the different equivalence ratios and mixtures, the maximum flame speed is given for the smaller flame size when it begins to propagate. This speed gradually decreases until the flame front reaches with the walls of the chamber and extinguishes.

The same trend is observed when the flame speed is represented versus the stretch rate (Figure 13iii). As the equivalence ratio increases, for the same rate of stretch of the flame, the flame speed increases. These curves also have a first section in which the flame speed increases strongly with the stretch rate, and a final section in which the speed hardly depends on the stretching of the flame. It should be taken into account that the final part of these curves, corresponding to the highest stretch rates, refers to the start of the combustion; that is, the start of the flame front leads to the highest stretch rates, and as the radius increases, stretch decreases.

5. COMPARISON OF THE RESULTS IN THE SPHERICAL AND CYLINDRICAL BOMBS

Once the results obtained in the spherical and cylindrical combustion bombs have been presented, it is interesting to make a comparison between the burning velocities obtained by each method. In this way, the appropriate conclusions about the influence of their geometry in the development of the combustion process can be drawn. The burning velocity u_l^p obtained in the SphCVCB is compared with the unstretched velocity u_l obtained with the image analysis in the CylCVCB in Figure 14, where a good agreement between both methodologies can be seen.

To study the influence of the equivalence ratio, pressure and temperature are fixed (0.1 MPa and 300 K) and the equivalence ratio is varied from 0.5 to 1 for the five compositions of the mixture, see Figure 14ii. It is also interesting to verify that the smallest differences occur for the 6.7% H_2 mixture. This is because, as already mentioned in the corresponding section, higher hydrogen contents in the mixture favor the instability of the flame and increase the surface roughness. This irregularity of the flame front makes it difficult for the image algorithm to obtain the radius during the analysis of the combustion video.

6. CONCLUSIONS

Combustion of synthesis gas has been characterized through blends of its main constituents, hydrogen and carbon monoxide. The tested blends have H_2 percentages of 0, 6.7, 25, 50, 80, and 100%, therefore covering the full range of the most typical syngas compositions. In addition, the fuel/air equivalence ratio of these mixtures has been varied from 0.5 to stoichiometry, a range that is interesting for the subsequent application in internal combustion engines, since these values would allow fuel savings (lean conditions) and the compatibility with post-treatment systems for pollutant emissions (stoichiometry).

Two constant volume combustion bombs have been used for carrying out the experiments. One bomb has a spherical geometry, where a two-zone diagnosis model has been used to process the obtained data. The second one is a cylindrical bomb with optical accesses through which the combustion process can be visualized and recorded using the Schlieren technique to subsequently treat the images obtained and thus obtain different characteristic variables of the process.

From the results obtained in the spherical combustion pump, several conclusions have been derived. With respect to the mixture composition, it has been found that the hydrogen content enhances the rate of combustion and the maximum pressure obtained. These same effects are obtained when the fuel/air equivalence ratio increases. In addition, some correlations between burning velocity, pressure, and temperature (type Metghalchi and Keck) have been obtained for each fuel/air mixture (eqs 2−4 and 5−7). It has been observed that both burning velocity at the reference conditions and the temperature exponent increase with the hydrogen content of the mixture and with the equivalence ratio, while the pressure exponent remains practically constant. Finally, the results have been corroborated and validated by comparing with other literature results.

The flame speed is determined using the optical method in the cylindrical bomb, where from the evolution of the flame front radius, the laminar burning velocity is obtained. These

https://dx.doi.org/10.1021/acs.energyfuels.0c03598
Energy Fuels 2021, 35, 3497−3511

results are consistent with those obtained and validated in the spherical bomb (using pressure evolution and the diagnosis model).

Finally, the comparison of the results obtained in the spherical and cylindrical combustion chambers has been made, obtaining a good agreement between both values. Results have also been compared and validated in Figure 7 with past results, which have been obtained by different authors of the bibliography using the same H_2/CO blends at the same conditions.

AUTHOR INFORMATION

Corresponding Author

M. Reyes − *Department of Energy and Fluid-Mechanics Engineering, University of Valladolid, Valladolid E-47011, Spain*; orcid.org/0000-0003-0993-7361; Email: miriam.reyes@uva.es

Authors

F.V. Tinaut − *Department of Energy and Fluid-Mechanics Engineering, University of Valladolid, Valladolid E-47011, Spain*

B. Giménez − *Department of Energy and Fluid-Mechanics Engineering, University of Valladolid, Valladolid E-47011, Spain*

A. Camaño − *Department of Energy and Fluid-Mechanics Engineering, University of Valladolid, Valladolid E-47011, Spain*

Complete contact information is available at: https://pubs.acs.org/10.1021/acs.energyfuels.0c03598

Notes

The authors declare no competing financial interest.

ACKNOWLEDGMENTS

The authors would like to thank the Spanish Ministry of Science and Innovation-Agencia Estatal de Investigación, for the financial support of this investigation with the research project PID2019-106957RB-C22. This work was developed under the support of the Research Group in Engines and Renewable Energies (MyER) from the University of Valladolid.

NOMENCLATURE

CIE = compression ignition engines
CNG = compressed nagural Gas
CylCVCB = cylindrical constant volume combustion bomb
ICE = internal combustion engines
NG = natural gas
RICE = reciprocating internal combustion engines
SphCVCB = spherical constant volume combustion bomb
SIE = spark ignition engine
L_b = Markstein length
p = pressure
T = temperature
α = temperature coefficient in the burning velocity
β = pressure coefficient in the burning velocity
ϕ = fuel/air equivalence ratio
R_f = flame front radio
S_L = unstretched flame propagation speed
S_n = stretched flame propagation speed (dR_f/dt)
U_L^p = laminar burning velocity (obtained in the SphCVCB with pressure register)
u_L = laminar burning velocity (obtained with Schlieren tecnique in the CylCVCB)

REFERENCES

(1) Payri González, F.; Desantes Fernández, J. M. *Motores de combustión interna alternativos*; Colección Académica Editorial UPV: 2011.

(2) Dinçer, İ.; Zamfirescu, C.. *Advanced power generation systems*; Academic Press: 2014.

(3) Ravi, K.; Mathew, S.; Bhasker, J. P.; Porpatham, E. Gaseous alternative fuels for Spark Ignition Engines-A technical review. *J. Chem. Pharm. Sci.* **2017**, *10*, 93−99.

(4) Muñoz, M.; Moreno, F.; Morea-Roy, J.; Ruiz, J.; Arauzo, J. Low heating value gas on spark ignition engines. *Biomass Bioenergy* **2000**, *18*, 431−439.

(5) Saravanan, N.; Nagarajan, G. An experimental investigation of hydrogen-enriched air induction in a diesel engine system. *Int. J. Hydrogen Energy* **2008**, *33*, 1769−1775.

(6) Karim, G. A. Hydrogen as a spark ignition engine fuel. *Hem. Ind.* **2002**, *56*, 256−263.

(7) Verhelst, S.; Sierens, R. Hydrogen engine-specific properties. *Int. J. Hydrogen Energy* **2001**, *26*, 987−990.

(8) Ji, C.; Wang, S. Effect of hydrogen addition on lean burn performance of a spark-ignited gasoline engine at 800 rpm and low loads. *Fuel* **2011**, *90*, 1301−1304.

(9) Tinaut, F. V.; Melgar, A.; Giménez, B.; Reyes, M. Prediction of performance and emissions of an engine fuelled with natural gas/hydrogen blends. *Int. J. Hydrogen Energy* **2011**, *36*, 947−956.

(10) Schefer, R. W.; Wicksall, D. M.; Agrawal, A. K. Combustion of hydrogen-enriched methane in a lean premixed swirl-stabilized burner. *Proc. Combust. Inst.* **2002**, *29*, 843−851.

(11) Das, L. M.; Gulati, R.; Gupta, P. K. A comparative evaluation of the performance characteristics of a spark ignition engine using hydrogen and compressed natural gas as alternative fuels. *Int. J. Hydrogen Energy* **2000**, *25*, 783−793.

(12) Bosch, C.; Wild, W. Process of producing hydrogen. U.S. Patent No. 1,115,776, Google Patents, 1914.

(13) Ji, C.; Dai, X.; Ju, B.; Wang, S.; Zhang, B.; Liang, C.; et al. Improving the performance of a spark-ignited gasoline engine with the addition of syngas produced by onboard ethanol steaming reforming. *Int. J. Hydrogen Energy* **2012**, *37*, 7860−7868.

(14) Hagos, F. Y.; Aziz, A. R. A.; Sulaiman, S. A. Syngas (H_2/CO) in a spark-ignition direct-injection engine. Part 1: Combustion, performance and emissions comparison with CNG. *Int. J. Hydrogen Energy* **2014**, *39*, 17884−17895.

(15) Shah, A.; Srinivasan, R.; To, S. D. F.; Columbus, E. P. Performance and emissions of a spark-ignited engine driven generator on biomass based syngas. *Bioresour. Technol.* **2010**, *101*, 4656−4661.

(16) Lee, H. C.; Jiang, L. Y.; Mohamad, A. A. A review on the laminar flame speed and ignition delay time of Syngas mixtures. *Int. J. Hydrogen Energy* **2014**, *39*, 1105−1121.

(17) Bouvet, N.; Chauveau, C.; Gökalp, I.; Halter, F. Experimental studies of the fundamental flame speeds of syngas (H_2/CO)/air mixtures. *Proc. Combust. Inst.* **2011**, *33*, 913−920.

(18) Dong, C.; Zhou, Q.; Zhao, Q.; Zhang, Y.; Xu, T.; Hui, S. Experimental study on the laminar flame speed of hydrogen/carbon monoxide/air mixtures. *Fuel* **2009**, *88*, 1858−1863.

(19) Fu, J.; Tang, C.; Jin, W.; Thi, L. D.; Huang, Z.; Zhang, Y. Study on laminar flame speed and flame structure of syngas with varied compositions using OH-PLIF and spectrograph. *Int. J. Hydrogen Energy* **2013**, *38*, 1636−1643.

(20) Sun, H.; Yang, S. I.; Jomaas, G.; Law, C. K. High-pressure laminar flame speeds and kinetic modeling of carbon monoxide/hydrogen combustion. *Proc. Combust. Inst.* **2007**, *31*, 439−446.

(21) Hassan, M. I.; Aung, K. T.; Faeth, G. M. Properties of Laminar Premixed CO/H_2/Air Flames at Various Pressures. *J. Propulasion Power* **1997**, *13*, 239−245.
(22) Natarajan, J.; Lieuwen, T.; Seitzman, J. Laminar flame speeds of H_2/CO mixtures: effect of CO_2 dilution, preheat temperature, and pressure. *Combust. Flame* **2007**, *151*, 104−119.
(23) Singh, D.; Nishiie, T.; Tanvir, S.; Qiao, L. An experimental and kinetic study of syngas/air combustion at elevated temperatures and the effect of water addition. *Fuel* **2012**, *94*, 448−456.
(24) He, Y.; Wang, Z.; Weng, W.; Zhu, Y.; Zhou, J.; Cen, K. Effects of CO content on laminar burning velocity of typical syngas by heat flux method and kinetic modeling. *Int. J. Hydrogen Energy* **2014**, *39*, 9534−9544.
(25) Jiang, Y.-h.; Li, G.-x.; Li, H.-m.; Zhang, G.-p.; Lv, J.-c. Study on the effect of hydrogen fraction on the premixed combustion characteristics of syngas/air mixtures. *Energy* **2020**, *200*, 117592.
(26) Jiang, Y.-h.; Li, G.-x.; Li, H.-m.; Zhang, G.-p.; Lv, J.-c. Experimental study on the Influence of Hydrogen Fraction on Self-acceleration of H_2/CO/air laminar premixed flame. *Int. J. Hydrogen Energy* **2020**, *45*, 2351−2359.
(27) Jiang, Y.-h.; Li, G.-x.; Li, H.-m.; Zhang, G.-p.; Lv, J.-c. Experimental Study on the Self-Similar Propagation of H_2/CO/Air Turbulent Premixed Flame. *Energy Fuels* **2019**, *33*, 12736−12741.
(28) Krejci, M. C.; Mathieu, O.; Vissotski, A. J.; Ravi, S.; Sikes, T. G.; Petersen, E. L.; et al. Laminar flame speed and ignition delay time data for the kinetic modeling of hydrogen and syngas fuel blends. *J. Eng. Gas Turbines Power* **2013**, *135*, No. 021503.
(29) Kéromnès, A.; Metcalfe, W. K.; Heufer, K. A.; Donohoe, N.; Das, A. K.; Sung, C.-J.; et al. An experimental and detailed chemical kinetic modeling study of hydrogen and syngas mixture oxidation at elevated pressures. *Combust. Flame* **2013**, *160*, 995−1011.
(30) Prathap, C.; Ray, A.; Ravi, M. R. Investigation of nitrogen dilution effects on the laminar burning velocity and flame stability of syngas fuel at atmospheric condition. *Combust. Flame* **2008**, *155*, 145−160.
(31) Burbano, H. J.; Pareja, J.; Amell, A. A. Laminar burning velocities and flame stability analysis of H_2/CO/air mixtures with dilution of N_2 and CO_2. *Int. J. Hydrogen Energy* **2011**, *36*, 3232−3242.
(32) Wang, J.; Huang, Z.; Kobayashi, H.; Ogami, Y. Laminar burning velocities and flame characteristics of $CO−H_2−CO_2−O_2$ mixtures. *Int. J. Hydrogen Energy* **2012**, *37*, 19158−19167.
(33) Bradley, D.; Gaskell, P. H.; Gu, X. J. Burning velocities, Markstein lengths, and flame quenching for spherical methane-air flames: a computational study. *Combust. Flame* **1996**, *104*, 176−198.
(34) Huang, Z.; Zhang, Y.; Zeng, K.; Liu, B.; Wang, Q.; Jiang, D. Measurements of laminar burning velocities for natural gas−hydrogen−air mixtures. *Combust. Flame* **2006**, *146*, 302−311.
(35) Tinaut, F. V.; Reyes, M.; Giménez, B.; Pastor, J. V. Measurements of OH* and CH* Chemiluminescence in Premixed Flames in a Constant Volume Combustion Bomb under Autoignition Conditions. *Energy Fuels* **2011**, *25*, 119−129.
(36) Reyes, M.; Tinaut, F. V.; Horrillo, A.; Lafuente, A. Experimental characterization of burning velocities of premixed methane-air and hydrogen-air mixtures in a constant volume combustion bomb at moderate pressure and temperature. *Appl. Therm. Eng.* **2018**, *130*, 684−697.
(37) Tinaut, F. V.; Reyes, M.; Melgar, A.; Giménez, B. Optical characterization of hydrogen-air laminar combustion under cellularity conditions. *Int. J. Hydrogen Energy* **2019**, *44*, 12857−12871.
(38) Bradley, D.; Hicks, R. A.; Lawes, M.; Sheppard, C. G. W.; Woolley, R. The measurement of laminar burning velocities and Markstein numbers for iso-octane−air and iso-octane−n-heptane−air mixtures at elevated temperatures and pressures in an explosion bomb. *Combust. Flame* **1998**, *115*, 126−144.
(39) Okafor, E. C.; Hayakawa, A.; Nagano, Y.; Kitagawa, T. Effects of hydrogen concentration on premixed laminar flames of hydrogen−methane−air. *Int. J. Hydrogen Energy* **2014**, *39*, 2409−2417.
(40) Metghalchi, M.; Keck, J. C. Burning velocities of mixtures of air with methanol, isooctane, and indolene at high pressure and temperature. *Combust. Flame* **1982**, *48*, 191−210.
(41) Han, M.; Ai, Y.; Chen, Z.; Kong, W. Laminar flame speeds of H_2/CO with CO_2 dilution at normal and elevated pressures and temperatures. *Fuel* **2015**, *148*, 32−38.
(42) Shang, R.; Zhang, Y.; Zhu, M.; Zhang, Z.; Zhang, D.; Li, G. Laminar flame speed of CO_2 and N_2 diluted H_2/CO/air flames. *Int. J. Hydrogen Energy* **2016**, *41*, 15056−15067.
(43) Li, Y.; Jia, M.; Liu, Y.; Xie, M. Numerical study on the combustion and emission characteristics of a methanol/diesel reactivity controlled compression ignition (RCCI) engine. *Appl. Energy* **2013**, *106*, 184−197.
(44) Li, H.-M.; Li, G.-X.; Sun, Z.-Y.; Zhou, Z.-H.; Li, Y.; Yuan, Y. Effect of dilution on laminar burning characteristics of $H_2/CO/CO_2$/air premixed flames with various hydrogen fractions. *Exp. Therm. Fluid Sci.* **2016**, *74*, 160−168.
(45) Burke, M. P.; Chen, Z.; Ju, Y.; Dryer, F. L. Effect of cylindrical confinement on the determination of laminar flame speeds using outwardly propagating flames. *Combust. Flame* **2009**, *156*, 771−779.
(46) Zhang, Y.; Shen, W.; Fan, M.; Zhang, H.; Li, S. Laminar flame speed studies of lean premixed H_2/CO/air flames. *Combust. Flame* **2014**, *161*, 2492−2495.

https://dx.doi.org/10.1021/acs.energyfuels.0c03598
Energy Fuels 2021, 35, 3497−3511